Proceedings Kenya Geothermal Congress 2024.
Nairobi, Kenya, 16 – 18, July 2024.

Application of supersonic ejectors to induce flow from low-pressure geothermal production wells

Daniel Wanga Odongo[1], Ximena Guardia Muguruza[2], Gunnar Dagur Jónsson[2], Guðrún Sævarsdóttir[2], Yonatan Afework Tesfahunegn[2], Ragnar Lárusson[2], María Sigríður Guðjónsdóttir[2]

[1]Kenya Electricity Generating Company PLC, Kenya; [2]Reykjavik University, Iceland

Keywords

Supersonic ejector, low-pressure wells, geothermal power

ABSTRACT

Geothermal wells are one of the key components and most capital-intensive parts of any geothermal power generation facility. However, they often experience pressure decline over their lifetime, leading in some cases to the well pressure falling below the power plant operating conditions, which make wells unsuitable for power generation. This can make the overall project more costly since additional wells must be drilled to compensate for the unavailable wells to maintain the desired power plant output. This study explores the possibility of using ejectors to solve that problem.

Ejectors have been used in various applications in oil and gas (Andreussi et al, 2003) and refrigeration (Manoj and Lijo, 2021). In geothermal power generation, ejectors are widely used to extract non-condensable gases from the condenser. A Study by Strusnik et al (2016) has shown how this can be improved further by controlling the gas extraction rate.

Supersonic ejectors are devices that use kinetic energy from a high-pressure stream to induce flow from a lower-pressure stream. Ejector parts are convergent-divergent nozzle, a suction chamber, a mixing section, and a diffuser. The high-pressure primary flow is accelerated through the nozzle throat reaching sonic conditions and inducing low pressure at the nozzle exit at supersonic conditions. This low-pressure zone allows the low-pressure secondary flow to entrain into the mixing chamber. Mixing of the flows occurs by pressure recovery in a following diffuser region when the mixture is decelerated to subsonic conditions again.

The experiments described in this paper were carried out to test a supersonic ejector on a laboratory-scale setup to connect two streams of saturated steam at different pressures to validate the analytical model developed by Andal (2023) and based on models by Huang et al (1999). Earlier works have shown that the dimensions of the ejector parts influence performance. This experiment was carried out for 5mm, 7mm and 9mm diameters of the constant area mixing section (CAMS). The results show that the 5mm CAMS provided the best results.

1. INTRODUCTION

After drilling and testing geothermal wells, their operating pressure determines if they can be connected to the steam-gathering system for power generation. Some wells indicate low pressure during testing and may not be able to feed fluid at sufficient pressure into the steam-gathering system. Others may have sufficient pressure to be used, however, over their lifetime the pressure declines and may fall below the power plant's operating level making them unusable. This would require drilling of additional (make-up) wells to cover the steam shortfall, which leads to considerable cost of drilling.

Wells are one of the most expensive items in geothermal power projects with an estimated of 34% by ESMAP (2012) and 32-37% of the total capital cost by Gehringer and Loksha (2012). By March 2024, Olkaria geothermal field located in Kenya, has 30 wells with pressures below the steam gathering system pressure, to the extent that they cannot provide steam for power generation. They are interconnected with higher-pressure wells that suppress them and, therefore, are kept shut or used for reinjection and field monitoring.

The unavailability of output from the shut-in wells means that the power plants are not able to generate at full capacity, especially when some wells are closed for maintenance. The requirement for more make-up wells to offset the shortfall also increases costs in drilling, connection of the wells, and field monitoring.

This problem could potentially be solved by supersonic ejectors, which are devices that use kinetic energy from a high-pressure stream to induce flow from a lower-pressure stream. They consist of a convergent-divergent nozzle, a suction chamber, a mixing section, and a diffuser (Figure 1). The high-pressure primary flow is accelerated through the nozzle throat reaching sonic conditions and inducing low pressure at the nozzle exit at supersonic conditions. This low-pressure zone allows the low-pressure secondary flow to entrain into the constant area mixing section. Mixing of the flows occurs followed by pressure recovery in the diffuser region when the mixture is decelerated to subsonic conditions. Varga et al (2009) and Ding Z. et al (2016) discuss ejector dimensions as key factors that determine their performance.

A typical ejector profile is shown in Figure 1.

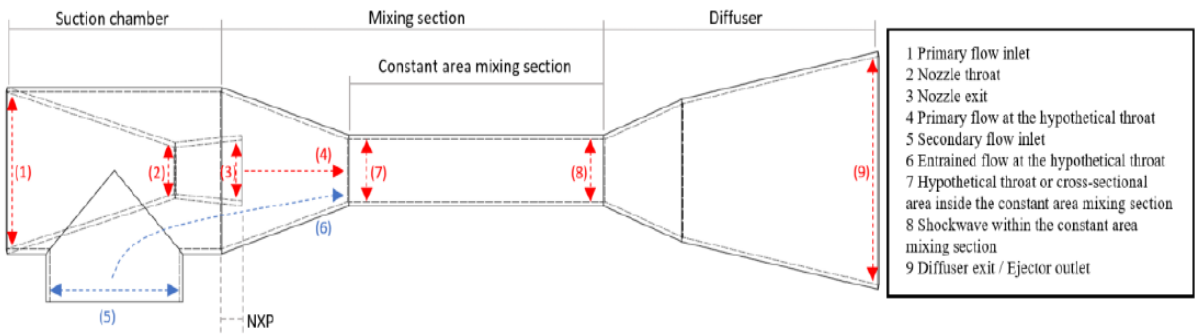

Figure 1: Profile of supersonic ejector profile (Andal, 2023)

Most of the wells in Olkaria that have experienced pressure declines are close to high-pressure wells in use that may be suitable for connecting using ejectors. Table 1 shows some of the possible well combinations that can be used.

Table 1: Olkaria wells that can be connected using ejectors.

Field	Well	Max flow pressure, bar-a	Mass flow, kg/s	Enthalpy, kJ/kg	Notes
Olkaria East	11A	15	22.2	1732	High pressure well in use
	36	5	11.7	2209	Shut after pressure decline
	36A	5	6.5	1981	Shut after pressure decline
Olkaria North-East	742A	17	11.4	2336	High pressure well in use
	709	14	21.9	1568	High pressure well in use
	706	6	34.5	1145	Intermittent use due to pressure decline
	710	4	18.6	1400	Shut after pressure decline
	712	5	9.7	2047	Intermittent use due to pressure decline
	713	5	15.8	2760	Intermittent use due to pressure decline
Olkaria Domes	912	15	15.5	2200	High pressure well in use
	912A	5	12.0	1800	Intermittent use due to pressure decline

In 2021, the power company Landsvirkjun tested a rudimentary ejector at its Theistareykir Geothermal Power Plant in Northeast Iceland to see if the high-pressure fluid from well ThG-11 could induce flow from the low-pressure well ThG-15. The tested ejector had a convergent nozzle but did not have a constant area mixing section to mix the primary and secondary streams properly. Despite that, entrained flow from the low-pressure well was observed, and an average of 1.69 MW of useful work was obtained using the ejector under the test conditions. However, it was found that the existing design of the ejector cannot handle the actual operating conditions of the wells for the plant, as the pressure difference between the nozzle outlet and entrained fluid is expected to be more significant and a higher back pressure is required (Guardia Muguruza, et al., 2023).

As part of the Geoejector project at Reykjavik University, Iceland, a laboratory size supersonic ejector has been designed and manufactured based on an analytical model developed in earlier work by Andal (2023) to improve the performance of the ejector at the Theistareykir Geothermal Power Plant.

This work outlines an experiment carried out to confirm the functioning of the supersonic ejector and validate the analytical model for supersonic ejectors developed by Andal, 2023. It focuses on the assessment of the ejector performance of a supersonic ejector by varying the constant area mixing section (CAMS) diameter. This will further contribute to ongoing research on the validation of the analytical and CFD models developed within the Geoejector project, as well as the use of ejectors for combining high and low-pressure geothermal wells in Olkaria, Kenya to maximize the use of the wells despite pressure declines.

2. METHODOLOGY

2.1 Ejector design

A design of a supersonic ejector on a laboratory scale was made using the analytical model developed by Andal (2023). This ejector was designed for a primary flow entering at 7 bar-g pressure, 212°C, and a mass flow of 0.005 kg/s; and a secondary flow entering at 2 bar-g pressure, 168°C, and a mass flow of 0.003 kg/s. To assess the effect of the diameter of the constant area mixing section on the performance of the ejector, three ejectors were made with different CAMS: 5 m, 7 mm, and 9 mm. Figure 2 shows the drawing of the ejectors designs and Table 2 shows their dimensions.

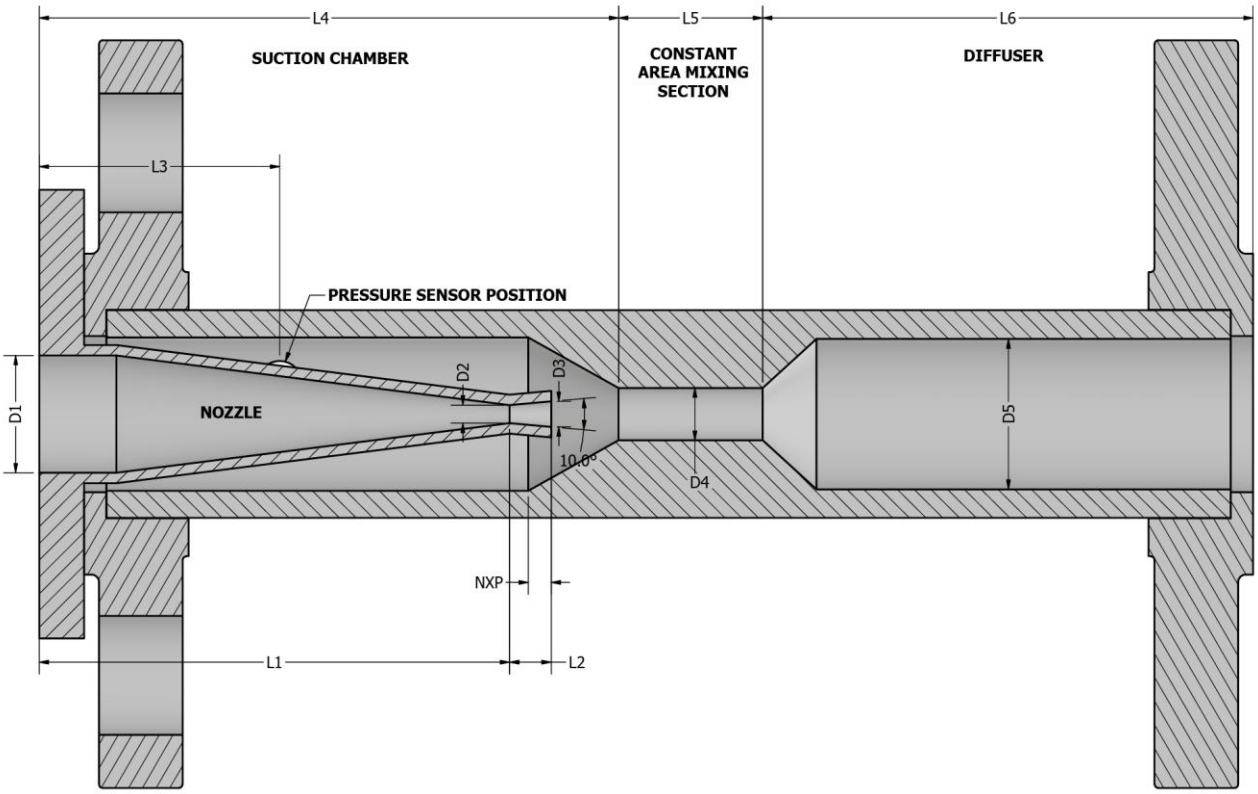

Figure 2. Drawing of the ejector's design, the main dimensions are shown in Table 2

Table 2: Dimensions of ejectors used in the laboratory experiments.

Ejector type	D1 (mm)	D2 (mm)	D3 (mm)	D4 (mm)	D5 (mm)	L1 (mm)	L2 (mm)	L3 (mm)	L4 (mm)	L5 (mm)	L6 (mm)	NXP (mm)
5 mm CAM	15.7	2.44	3.41	5	20	63	5.57	32.2	75.2	21.2	65.7	3.07
7 mm CAM	15.7	2.44	3.41	7	20.1	63	5.57	32.2	77.6	19.3	65.7	3.07
9 mm CAM	15.7	2.44	3.41	9	19.8	63	5.57	32.2	64	19.6	66.7	4.57

2.2 Equipment

A 22-kW boiler produced the primary steam flow at 7 bar and 2120°C, whereas a 39 kW was used for the secondary steam flow production at 2 bar and 160°C (see Figure 3).

a **b**

Figure 3. Boilers used for laboratory experiments. Note: a. 22 kW boiler, b. 39 kW boiler

Additionally, two separators were used in the experiments to remove the water from the steam flow (Figure 4).

Figure 4. Separators used for the laboratory experiments.

2.3 Measurement devices

Pressure, temperature, and mass flow sensors were used in the experiment. Table 3 shows their models.

Table 3: Characteristics of the sensor used in the experiment.

Device	Model	Amount	**Photo**
Pressure sensors	PCE-28/EXD type	3	
Micro pressure sensor	JC91 type	1	
Pressure gauge	EN 837-1	1	

Device	Model	Amount	Photo
Temperature sensor	STA 206 P-type	4	
Vortex flow meter	Model Endress D 200	1	

2.4 Schematic of the experiment

Figure 5 shows the setup for the experiments, which include two boilers for steam generation for the primary and secondary flows; a separator to remove water residuals from the primary flow; pressure sensors, temperature sensors, and a flow meter, to measure pressure, temperature, and mass flow, respectively; and the manufactured ejector. Also, air pressure regulators were included to test leakages with air before the steam tests. The setup is shown in Figure 6.

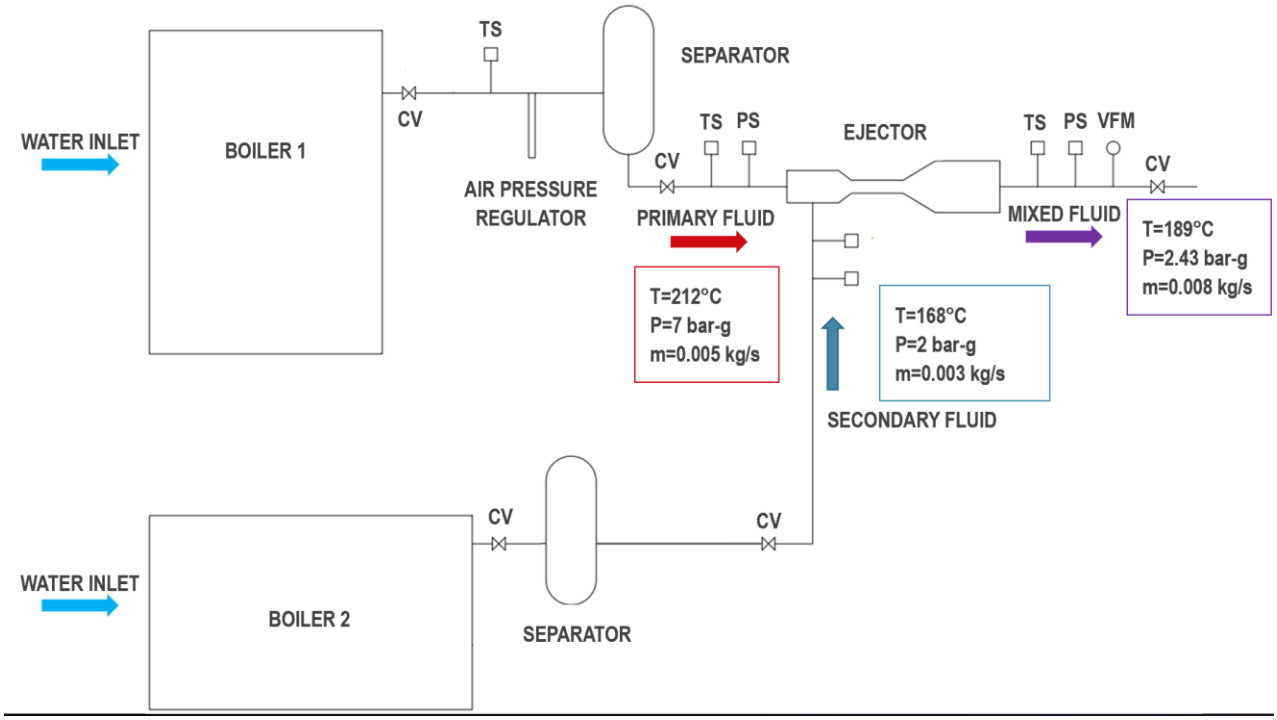

Figure 5. Schematic of the set-up used for laboratory experiments.

Note: CV=Control valve, PS=Pressure sensor, TS= Temperature sensor, VMF=Vortex flow meter.

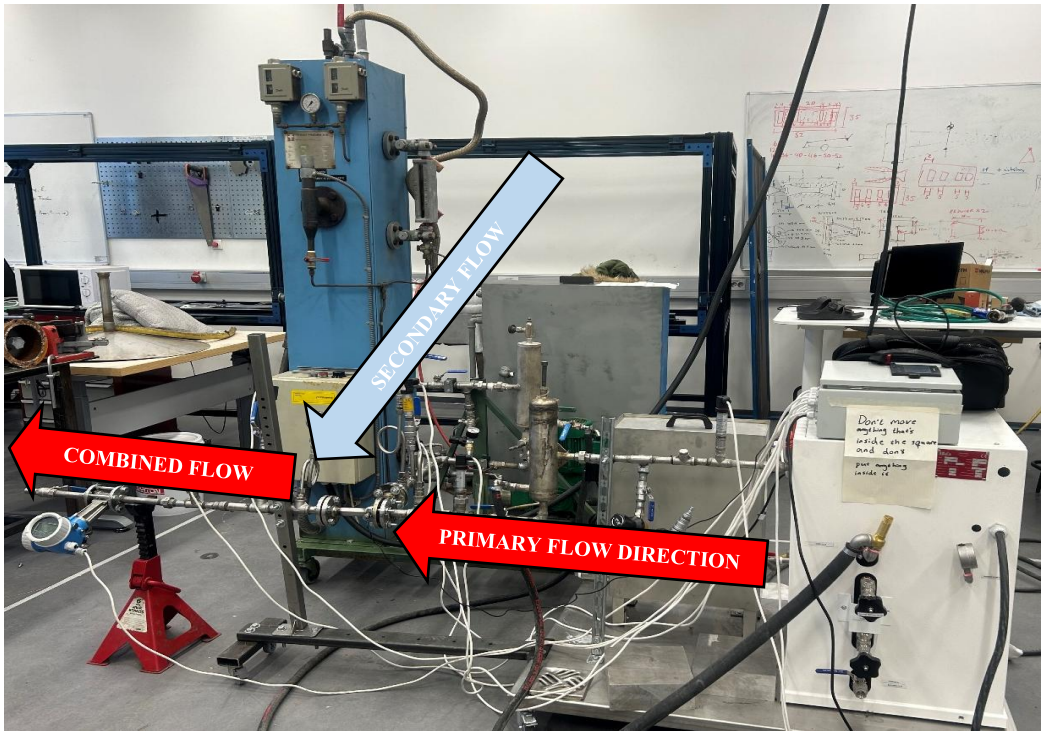

Figure 6. Set-up for laboratory experiments.

2.5 Description of the process of the experiments

The test started by opening the air pressure regulator valve in Figure 6 and using air pressure to test for leakages. For the leaking joints, pipes and unions were checked and tightened. Then, the water tanks for the two boilers were filled up.

Once the system was without leakages, the primary flow boiler was turned on, and the valve after the separator was kept open after the separator to release the water residuals. When pure steam was seen coming out from the separator outlet, the valve was closed. Then, we waited until the 7 bar-g operating pressure of the boiler was achieved, and the outlet valve of the system was partially? closed to reach a 2.5 bar-a measurement in the pressure gauge close to the ejector exit.

Once primary pressure was stable and pure steam observed at the outlet, the secondary flow boiler was turned on. The valve after the separator was kept open to release the water residuals. When pure steam was seen coming out from the separator outlet, the valve was closed. Then, we waited until the 2 bar-g operating pressure of the secondary flow boiler was achieved to start taking readings of mass flow, velocity, and temperature from the vortex flow meter every minute, and of pressure from the two boiler's pressure gauges in Figure 6. After ten minutes of readings, the boilers were turned off.

All the data from the sensors were stored on a PLC SD card, and after the measurements were made, these data were downloaded as CSV values and then processed in Microsoft Excel files. As all the sensors registered a 4-20mA signal, the recorded values were transformed to the desired units (bar, °C, and kg/s).

The experiment was carried out on three ejectors with constant area mixing sections (CAMS) of 9mm,7mm and 5 mm.

3. RESULTS AND DISCUSSION

Figure 7 shows the pressure and total mass flow obtained with the 5mm CAMS ejector during the test.

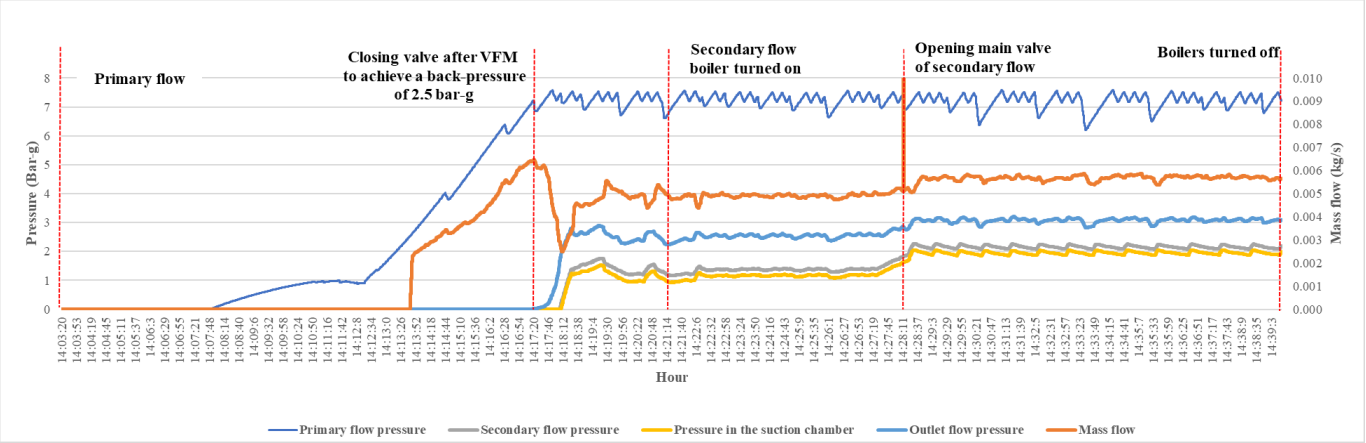

Figure 7. Pressure and total mass flow measured for the 5 mm CAMS ejector

Thie primary flow pressure plot shows there is a pressure drop from the primary flow as it goes through the nozzle, achieving a pressure in the suction chamber that is below the secondary flow pressure, which allows entraining of the secondary flow to the system. The primary flow pressure drop is from 7 to 1 bar-g on average. As the secondary flow pressure is 2 bar-g, it can be entrained into the system and mixed with the primary flow, resulting in an intermediate pressure at the outlet of the ejector of 3 bar-g at the outlet after pressure recovery.

It is observed that the mass flow increases at the outlet of the ejector which is a sign of entrainment of secondary flow into the primary flow. When there was just the primary flow, the mass flow was about 0.005 kg/s, but when the secondary flow entered the system, it increased to 0.0058 kg/s for the 5mm CAMS. Table 4 shows the average values of results from the experiment for the 9mm, 7mm and 5mm CAMS.

Table 4: Summary of results

CAMS (mm)	Primary flow pressure (bar-g)	Suction chamber pressure (bar-g)	Secondary flow pressure (bar-g)	Outlet pressure (bar-g)	Primary mass flow (kg/s)	Total mass flow (kg/s)
5	7.2	1.9	2.2	3.1	0.005	0.0058
7	7.2	1.9	2.1	2.7	0.005	0.0055
9	7.2	1.9	2.2	2.5	0.005	0.0049

A comparison of the results was made for the three CAMS based on the calculated induced pressure (Equation 1) and the calculated entrainment ratio (Equation 2) of the ejector. Induced pressure refers to the difference between the outlet pressure and the secondary pressure, while entrainment ratio refers to the ratio between the secondary mass flow and the primary mass flow.

$$Induced\ pressure = P_{outlet} - P_{secondary} \quad (1)$$

$$Entrainment\ ratio = \frac{\dot{m}_{secondary}}{\dot{m}_{primary}} \quad (2)$$

Where P_{outlet} , $P_{secondary}$, $\dot{m}_{primary}$, $\dot{m}_{secondary}$ are pressure at the outlet of the ejector (bar), pressure at inlet pressure of secondary flow (bar), primary mass flow (kg/s) and secondary mass flow (kg/s). Figure 8 shows the induced pressure obtained with the different CAMS ejectors.

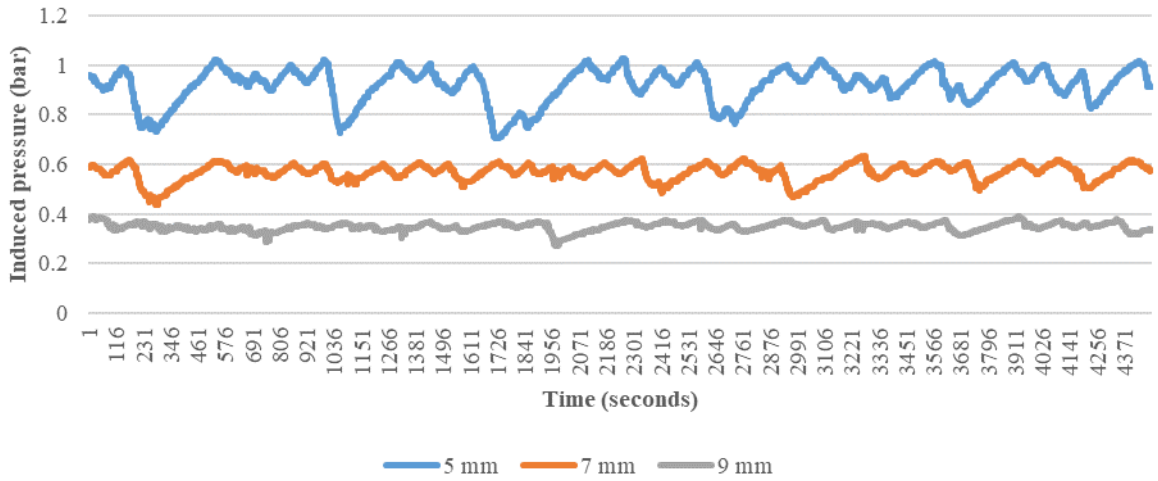

Figure 8. Induced pressure for different CAMS (5, 7, and 9 mm)

As can be noticed, the 5 mm CAMS ejector has the greatest induced pressure of the 3 ejectors, followed by the 7 mm ejector and finally the 9 mm ejector. This is consistent with the analytical model used for the ejector design, which predicted a better performance with a 4 mm CAMS ejector. The experiment has however not been done for the 4mm CAMS due to delays in procurement of required flanges. This will be done once the flanges are received.

Figure 9 shows the entrainment ratio obtained with the different CAM ejectors.

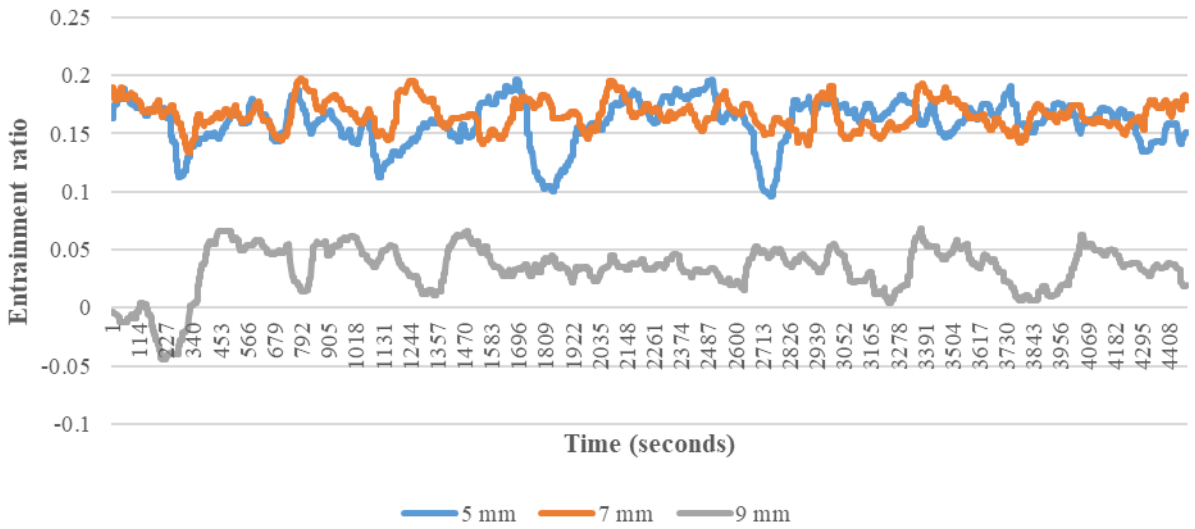

Figure 9. Entrainment ratio for different CAM (5, 7, and 9 mm)

As noticed from Figure 9, the 5- and 7-mm CAMS ejectors have entrainment ratios ranging from 0.1 to 0.2, whereas the 9 mm ejector has a much lower entrainment ratio, ranging from 0.01 to 0.07 and in some cases, negative values of entrainment were observed, suggesting backflow to the secondary flow entrance when there is not enough under pressure to be able to entrain the secondary flow.

4. CONCLUSIONS

- An experimental setup was developed to test three different CAMS ejectors for combining high and low-pressure steam flow.
- Preliminary tests of the 9mm, 7mm, and 5 mm CAMS ejectors with a supersonic nozzle, show that the three ejectors induce pressure from the secondary flow, however, the 5 mm CAMS ejector has the best performance inducing the highest induced pressure.
- The entrainment ratio is highest for the 5mm CAMS. However. entrainment ratios of the 5mm and 7mm CAMS ejector are very similar, however, a much lower entrainment ratio is observed for the 9 mm CAMS ejector, leading sometimes to backflow.
- Further experiments will be executed to validate the analytical and CFD models.
- After the validation of the models, they can be applied to the wells in Olkaria by designing a life-size version to combine low- and high-pressure wells and keep the wells in use despite their pressure falling below the steam field pressure.

REFERENCES

Andal J., Ragnar Lárusson R., Muguruza G, Sævarsdóttir G., Tesfahunegn Y., Júlíusson E., Sveinsson K, Chauhan V., Guðjónsdóttir M., Improvement of an Geoejector Design Using an Analytical Model and Data from Theistareykir Geothermal Field. Proceedings World Geothermal Congress, Beijing, China (2023).

Andal Jeffrey Macatangay. Geoejector: extracting geothermal fluid from a low-pressure geothermal well, MSc thesis, Reykjavík University, Reykjavik (2023).

Andreussi P., Sodini S., Faluomi V., Ciandri P., Ansiati A., Paone F., Battaia C., De Ghetto G, "Multiphase Ejector to Boost Production: First Application in the Gulf of Mexico," in Offshore Technology Conference, Houston, Texas (2003).

Gehringer, M. & Loksha, V.C. Geothermal Handbook: Planning and Financing Power Generation. Washington DC: World Bank Group, Energy Sector (2012)

Geothermal Handbook: Planning and Financing Power Generation, ESMAP Report No.: 002/12, (2012) https://www.esmap.org/sites/esmap.org

Huang, B., Chang, J., Wang, C., & Petrenko, V. A 1-D analysis of ejector performance, International Journal of Refrigeration, Pages 354–364 (1999)

Manoj P., Lijo V., "Recent developments in ejector refrigeration system," IOP Conf. Series: Materials Science and Engineering, vol. 1114 (2021).

Strušnik D, Golob M, Avsec J., "Effect of non-condensable gas on heat transfer in steam turbine condenser and modelling of ejector pump system by controlling the gas extraction rate through extraction tubes," Energy Conversion and Management, no. 126 (2016), pp. 228-246.

Szabolcs Varga, Armando C. Oliveira, Bogdan Diaconu. Influence of geometrical factors on steam ejector performance – A numerical assessment, international journal of refrigeration 32 (2009) 1694–1701, (2009).

Zhaoqiu Ding, Lei Wang, Hongxia Zhao, Hailun Zhang, Chen Wang. Numerical study and design of a two-stage ejector for subzero refrigeration, Applied Thermal Engineering 108 (2016) 436–448, (2016).

Guardia M., Andal J., Ragnar Lárusson R., Sævarsdóttir G., Tesfahunegn Y., Júlíusson E., Sveinsson K, Chauhan V., Guðjónsdóttir M., Connecting high- and low-pressure geothermal wells using an ejector: Analysis of first field tests at the Theistareykir Geothermal Power Plant Proceedings World Geothermal Congress, Beijing, China (2023).